Applied Catalysis B: Environmental 182 (2016) 123–131

Contents lists available at ScienceDirect

Applied Catalysis B: Environmental

journal homepage: www.elsevier.com/locate/apcatb

Influence of iridium oxide loadings on the performance of PEM water electrolysis cells: Part II – Advanced oxygen electrodes

Caroline Rozain[a,b], Eric Mayousse[a], Nicolas Guillet[a,*], Pierre Millet[b]

[a] Univ. Grenoble Alpes, F-38000 Grenoble, France; CEA, LITEN, F-38054 Grenoble, France
[b] Institut de Chimie Moléculaire et des Matériaux d'Orsay, Université Paris-Sud 11, Orsay, France

ARTICLE INFO

Article history:
Received 8 June 2015
Received in revised form 8 August 2015
Accepted 5 September 2015
Available online 9 September 2015

Keywords:
PEM water electrolysis
Low catalyst loading
Iridium oxide
Titanium particle
Ageing

ABSTRACT

The purpose of this research paper is to report on the applicability of micro-sized titanium particles as the support of IrO2 particles at the anode of PEM water electrolysis cells. A PEM single cell containing only 0.1 mg cm^{-2} of IrO2 as anode catalyst and 50 wt.% metallic Ti achieved 1.73 V at 1 A cm^{-2} and 80 °C. Such level of performance is similar to those usually obtained with conventional loadings of several mg cm^{-2} of IrO_2 at the anode side. SEM observations and EIS measurements revealed that the micro-sized titanium particles added to the anodic catalyst layer favor an intimate electrical contact between the catalyst layer and the current collector, and contribute to the reduction of the ohmic resistance of the catalytic layer. A long-term water electrolysis experiment using IrO_2/Ti as anode material demonstrated a good stability of the MEA over 1000 h of operation. Using such a low IrO_2 loading (0.1 mg cm^{-2} IrO_2), the degradation rate measured at 1 A cm^{-2} was reduced from 180 μV h^{-1} (measurement made on pure IrO_2 anode) down to only 20 μV h^{-1} for the 50 wt.% IrO_2/Ti anode.

1. Introduction

Nowadays, hydrogen is by far the most promising option as clean, carbon-free and efficient energy carrier. Proton exchange membrane (PEM) water electrolysis is now recognized as a promising water splitting technology because it produces clean hydrogen from water and transient power sources [1]. A major drawback of PEM water electrolysis is its cost that partly comes from the use of platinum-group metals (PGM) as electrocatalysts. PGM are required because of the acidic environment of perfluorosulfonic (PFSA) membrane materials used as solid electrolyte (the acidity of PFSA membranes such as Nafion® is roughly equivalent to that of 0.5 M H_2SO_4 aqueous solution [2]). Only PGM can withstand the aggressive oxidative environment of the process especially when operating at high current densities (high potential). Because of the scarcity and cost of PGM, a reduction of catalyst loadings while maintaining at the same time an acceptable level of performance is needed to make the technology most cost affordable.

The anode catalyst has been the focus of many studies on PEMWEs because the oxygen evolution reaction (OER) is the main source of irreversibility [3]. In state-of-the-art technology, pure IrO_2 is generally used as catalyst with typical loadings of a few mg cm^{-2} [4]. One method to reduce catalysts loading is to disperse catalyst nanoparticles at the surface of a conducting support of large surface area. The support enhances the dispersion of the active material, reduces the probability of catalyst particles agglomeration and thus favors the development of large active (electrochemical) surface areas [5–8]. In PEM fuel cell technology, catalysts loading have been significantly reduced by using high surface area carbonaceous conducting supports such as carbon powders [9], carbon nanofibers [10], and even carbon nanotubes [11,12]. However, the high anodic potential of operation of PEM water electrolysis anodes (≈1.5 V *vs.* RHE) proscribes the use of carbon-based materials as catalyst support because carbon is easily oxidized into carbon dioxide according to $C + 2H_2O \rightarrow CO_2 + 4H^+ + 4e^-$ at a potential of only 0.206 V *vs.* RHE [13,14]. Consequently, suitable support materials, alternative to carbonaceous materials, are necessary for application in PEM water electrolysers. In the literature, metal carbides such as TiC [15], TaC [16], SiC [17], doped [18] or reduced form [18–20] of titanium [7,21] or tin oxide [22,23] have been investigated as possible catalyst support. However, along with the instability of most of these supports in oxidizing environments [18,24], the noble metal loadings in these composite electrodes could not be reduced to less than 1–2 mg cm^{-2} in order to compensate the low electronic conductivity of these materials.

* Corresponding author at: Univ. Grenoble Alpes, F-38000 Grenoble, France; CEA, LITEN, F-38054 Grenoble, France.
E-mail address: nicolas.guillet@cea.fr (N. Guillet).

http://dx.doi.org/10.1016/j.apcatb.2015.09.011
0926-3373/

Abbreviations

A, dimensionless number Fitting parameter
B, Cm^{-2} Fitting parameter, capacity of a single layer of catalyst
η, % Efficiency
MEA Membrane electrodes assembly
m_{IrO_2}, $mg\,cm^{-2}$ IrO_2 loading of the electrode
m_{layer}, g Mass of a single layer of particles
LHV, J lower heating value of hydrogen ($244\,kJ\,mol^{-1}$)
Q^*, $C\,cm^{-2}$ Total charge accessible on the electrode
R, nm Spherical particle radius
ρ, $g\,cm^{-3}$ Density of IrO_2 ($11.66\,g\,cm^{-3}$)
RHE, V Reversible hydrogen electrode

Titanium is the most widely employed substrate of chlorine and/or oxygen evolution catalyst for dimensionally stable anodes (DSA® [25]) in the chlor-alkali industry [26–29]. A thin layer of titanium dioxide spontaneously forms at the surface of metallic titanium when exposed to air [30] and its thickness increases with oxygen pressure [31], applied current density [32] and temperature [31]. Since titanium dioxide is a semi-conductor of low electronic conductivity, metallic titanium seems to be an inadequate support of IrO_2 for application in PEM water electrolysis cells. However, Mazúr et al. have reported the possibility to overcome this lack of conductivity of non-conductive TiO_2 nanoparticles by using TiO_2/IrO_2 mixtures of sufficiently high IrO_2 percentage (>60 wt.% IrO_2/TiO_2 with an IrO_2 loading of $0.9\,mg\,cm^{-2}$) [33].

In the first part of this research paper (submitted to Appl. Catal. B), we reported results obtained with pure IrO_2 anodes containing low (between 0.1 and $2.6\,mg\,cm^{-2}$ IrO_2) catalyst loadings. Electrochemical characterizations showed that for unsupported particles, there is a threshold loading value of approximately $0.5\,mg\,cm^{-2}$ IrO_2 below which the percolation of IrO_2 particles is not sufficient and electrochemical performance tends to degrade rapidly. These results suggest that in the low IrO_2 loading range (<$0.5\,mg\,cm^{-2}$ IrO_2), there is a need to add a conductive support to the catalyst particles to compensate their lack of percolation and to keep a good electronic conductivity inside the active layer. The aim of the study reported here is to use micro-sized titanium particles to increase the conductivity of the anodic catalytic layer. The electrochemical properties of the IrO_2/Ti catalyst have been investigated in real PEM water electrolysis conditions using a single ($25\,cm^2$ area) cell.

2. Experimental

2.1. MEA preparation

A Nafion® NRE 115CS (DuPont™) membrane with a typical thickness of 127 μm was used as solid polymer electrolyte. A 50 wt.% IrO_2/Ti powder prepared as follows was used as OER electrocatalyst: a commercial iridium oxide (Surepure® Chemetals) was mechanically mixed with sieved titanium particles ($1.24 < \phi < 40$ μm, Aldrich). A commercial 46 wt.% Pt/carbon black (TEC10V50E, Tanaka Kikinzoku Inc.) was used as hydrogen evolution electrocatalyst at the cathode. Electrodes were prepared as follows: catalysts and Nafion ionomer (5 wt.% in water and ethanol, D520 DuPont™) mixtures were first ultrasonically suspended in a mixture of deionized water and isopropanol (volume ratio 1:1); catalytic suspensions thus obtained were then sprayed over flat PTFE sheets used as intermediate support; electrode layers ($25\,cm^2$) were then bonded on each side of the membrane by hot pressing at 135 °C and 4 MPa for 6 min. The Nafion content of the electrocatalytic layers was set to 5 and 26 wt.% for the anode and cathode, respectively. Catalyst loadings were accurately determined by weighting the PTFE support before and after the transfer of the active layers to the membrane. In all experiments reported in this paper, the cathode catalyst loading was kept constant at $0.25 \pm 0.01\,mg_{Pt}\,cm^{-2}$. After this, membrane-electrode assemblies (MEAs) thus obtained were treated for 1 h in 0.5 M sulfuric acid aqueous solution to completely exchange the membrane in proton form and remove any trace of possible chemical pollutant. Then, they were stored in deionized water ($18.2\,M\Omega\,cm^{-1}$) for 12 h. They were finally used for electrochemical characterization using a stainless steel electrolysis cell. MEAs were clamped between a porous titanium disc made of sintered powder (Applied Porous Technology Co., Sweden, mean pore size value ≈10 μm, see Fig. 1) at the anode side and a carbon—based gas diffusion layer (SGL group, Sigracet®-34 BC) at the cathode side. The cell was tightened between two stainless steel plates, using a dynamometric wrench to set the fastening screws at to 8 N m.

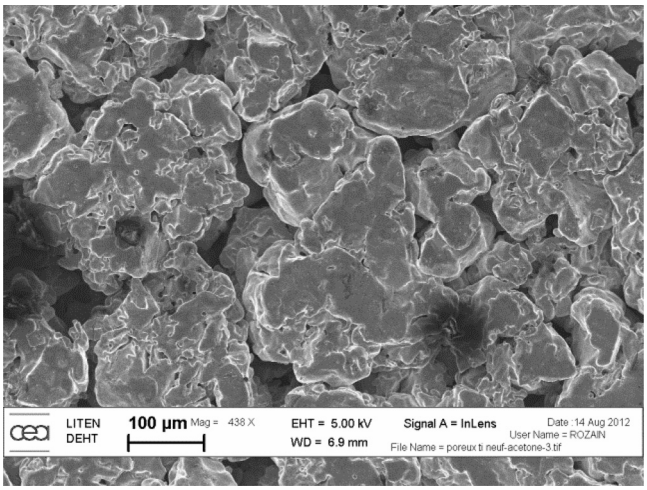

Fig. 1. SEM images of the porous titanium used as diffusion layer and anode current conductor.

2.2. Evaluation of PEMWE performances

50 wt.% IrO_2/Ti anodes containing various IrO2 loadings (ranging from 0.1 to $0.7\,mg\,cm^{-2}$ IrO_2) were prepared and then characterized using cyclic voltamperometry, electrochemical impedance spectroscopy (EIS) and by recording polarization curves. A series of thirteen MEAs was prepared and tested; all parameters (temperature, ionomer content, cathode and membrane) were kept constant except the IrO_2 loading.

Electrolysis performances were measured at a constant temperature of 80 °C and at atmospheric pressure. The temperature of deionized water circulating through the anodic compartment of the cell was kept at the same value as the temperature of the cell (to avoid temperature gradients). During experiments, only the anode was supplied with deionized water, at a constant flow rate of $200\,ml\,h^{-1}$. Before electrochemical characterization, the different electrodes were "activated" using the same procedure: during approximately 12 h, four polarization curves were recorded in the 0.04–2.00 $A\,cm^{-2}$ range, by applying $0.2\,A\,cm^{-2}$ step and 10 min stabilization for each step.

EIS measurements were carried out using a high current potentiostat (Bio-Logic Science Instruments SAS, HCP-803, 80 A) at frequencies ranging from 10 kHz down to 200 mHz. Measurement currents were the same as for the polarization curves; a stabilization period of 2 min for each step was applied in order to reach a quasi-stationary state. The amplitude of the sinus perturbation was carefully chosen for each current to fulfill the linearity condi-

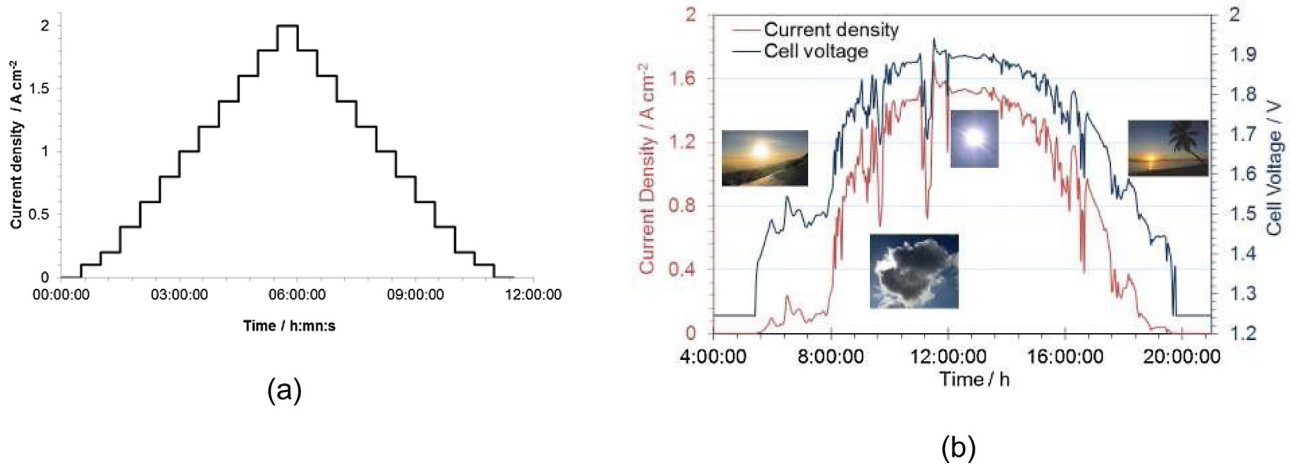

Fig. 2. Current density profiles used for ageing tests. (a) "Accelerated" ageing tests composed of a series of current steps from 0 to 2 A cm^{-2} and cell temperature set at 80 °C. (b) Real "solar"-type profile composed of a stand by phase, numerous and frequent variations of current. In this case, the cell temperature was set at 60 °C.

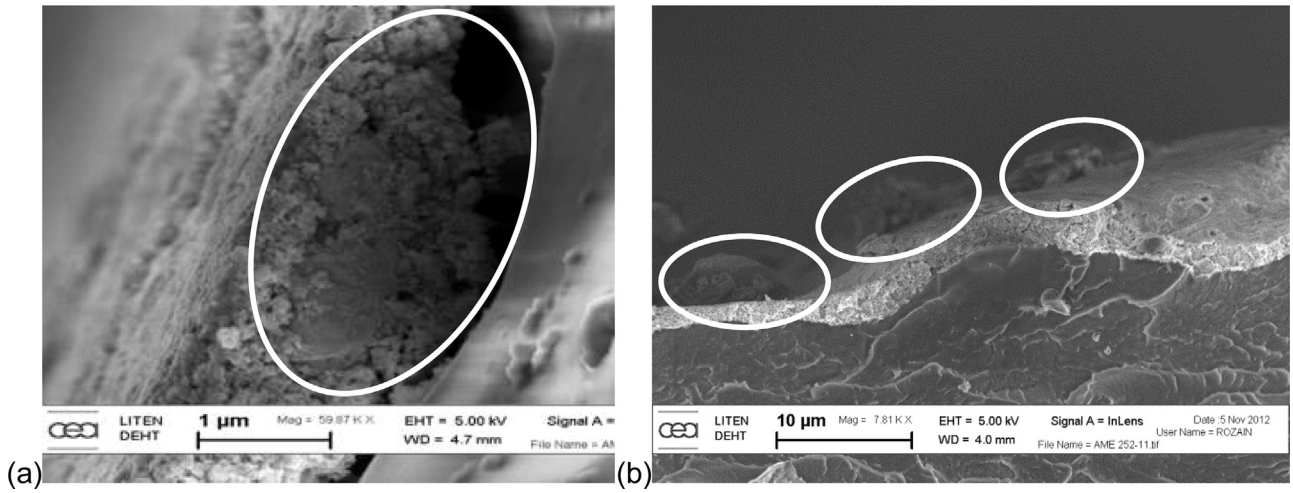

Fig. 3. SEM images of 50 wt.% IrO_2/Ti anode with 0.31 mg cm^{-2} IrO_2; (a) titanium particles whose diameter is less than the thickness of the electrode are located in the volume of the active layer while (b) the largest ones protrude from the surface.

tions of the system, while ensuring a sufficient signal/noise ratio. Experimental impedance spectra were fitted using a simple equivalent circuit ($L + R_{ohm} + R_1//Q_1 + R_2//Q_2$) composed by an inductance L (used to account for the inductance introduced by the wiring setup), in series with a resistance R_{ohm} (purely ohmic resistance of the cell due to current collectors, membrane, electrodes, and measurement device such as connectors and wires) and two different parallel circuits R//Q (where R is a charge transfer resistance and Q a constant phase element used to simulate the double layer capacitance). Even though this is not yet clearly demonstrated in the literature, the high frequency equivalent circuit $R_1//Q_1$ used in this model is attributed to reactions occurring at the cathode, and the low frequency equivalent circuit $R_2//Q_2$ is attributed to anodic reactions.

In order to evaluate the real active surface area of the electrodes, before and after ageing experiments, cyclic voltammograms (CVs) of the anodes were recorded using the cathode under H_2 atmosphere as reference electrode (RHE: H_2/Pt, at room temperature and atmospheric pressure) at different scan rates (from 5 to 100 mV s^{-1}) and between the potential limits of hydrogen and oxygen evolution reactions (0.05–1.3 V). All CVs were recorded at room temperature using a VSP2 Bio-Logic potentiostat.

Ageing tests of the PEMWE cells were performed using two different ageing protocols. Indeed, it is recognized in the literature that high current densities and elevated operating temperature accelerate the ageing of PEMWE components [34–36]. Then, we designed a specific "accelerated" ageing test protocol: a series of current steps (30 min long each), comprised between 0 and 2 A cm^{-2} (see Fig. 2a) was applied to the cell kept at 80 °C. However, such a test protocol is not representative of a real application comporting frequent power fluctuations (*e.g.*, due to the intermittent nature of the most renewable energy sources) and a succession of power on/off phases. Therefore, a second ageing test profile was also used. This is a 16 h long "solar" profile with a current density ranging from 0 to 1.7 A cm^{-2} (see Fig. 2b). During experiments, the cell temperature was set at 60 °C, a value commonly used by PEMWE manufacturers. For the two profiles, the two patterns were applied 6 times, and followed by EIS measurements and polarization curves as described before.

2.3. Physical characterizations

The particle size distribution of titanium nanoparticles used in the experiments was determined with a Malvern Mastersizer 3000® laser diffractometer. Post-mortem characterization of MEAs

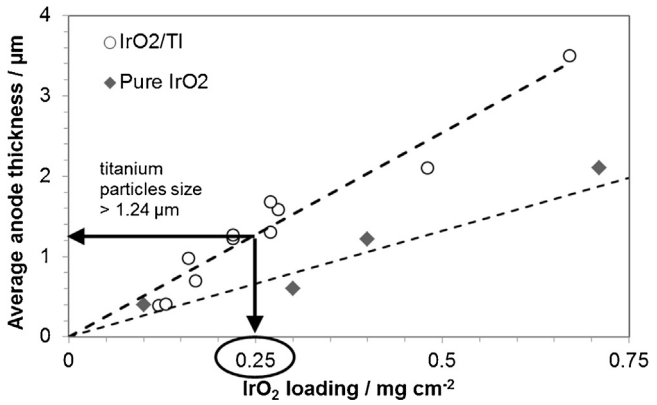

Fig. 4. Anode average thickness determined from SEM analysis on cryofractured MEAs as a function of IrO_2 loading.

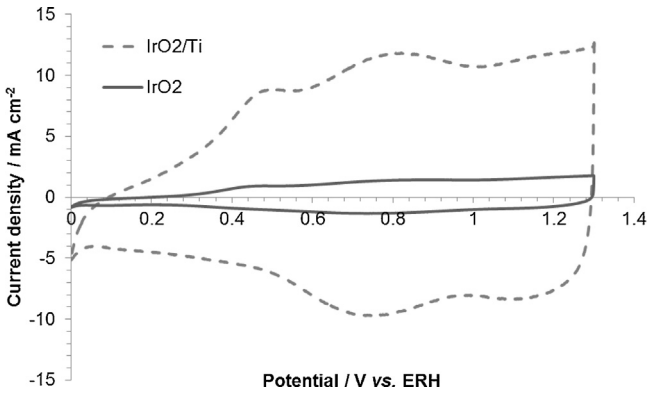

Fig. 5. Cyclic voltammograms of 50 wt.% IrO_2/Ti and IrO_2 anodes measured at 25 °C and 20 mV s^{-1}; IrO_2 loading for both electrodes was 0.3 mg cm^{-2} IrO_2.

with various IrO_2 loadings was carried out by scanning electron microscopy (SEM) analysis. MEAs cross sections were prepared by cryofracture and observed with a LEO 1530 field emission gun-scanning electron microscope (FEG-SEM) at an accelerating voltage of 5 kV under a high vacuum.

3. Results and discussion

3.1. Anode morphology

Typical SEM images of cryofractured MEAs after electrochemical ageing tests are shown in Fig. 3. The mean size of IrO_2 catalyst particle was found to be in the 15 nm range. We used titanium particles with a large distribution of size ($1.24 < \phi < 40$ µm). Small titanium particles are found embedded within the catalytic layer (Fig. 3a) and larger particles (those which have a diameter larger than the thickness of the catalytic layer) are found to protrude from the catalyst layer (Fig. 3b). Larger titanium particles penetrate inside the porosities of the porous titanium current collector (Fig. 1) and contribute to improve the electronic contact between the catalyst layer and the current collector. They also contribute to a better distribution of current lines within the catalytic layer.

In order to optimize the structure of the IrO_2/Ti catalytic layers, we measured their thickness as a function of IrO_2 loadings. Results are plotted in Fig. 4. The thickness tends to increase linearly with the IrO_2 loading for both IrO_2/Ti and pure IrO_2 particles electrodes. The catalytic layers prepared with IrO_2/Ti 50 wt.% are logically thicker than those prepared with pure IrO_2. Considering that the minimum Ti particles size used in these experiments is 1.24 µm, all Ti particles will protrude from the catalyst layer for a threshold value of 0.25 mg cm^{-2} IrO_2.

3.2. Influence of anode composition on the electrochemical active surface area of catalyst

Fig. 5 shows the cyclic voltammograms of two anodes prepared with the same amount of iridium oxide (0.3 mg cm^{-2} of IrO_2). The first one contains only unsupported IrO_2 nanoparticles, while the second one contains a 50 wt.% mixture of IrO_2/Ti. Both anodes show the typical redox behaviour characteristic of IrO_2 electrodes in this potential range [37]. However, the current density recorded on unsupported IrO_2 anode (and hence the associated coulombic charge) is much lower than what was recorded on the IrO_2/Ti anode (although the IrO_2 loading is the same in both cases).

The total voltammetric charges Q* of each electrode (a characteristic that is used to make comparison) were determined by integration of the CVs at different scan rates (5, 10, 20, 50 and 100 mV s^{-1}), as described in Part I of this research paper [38], using

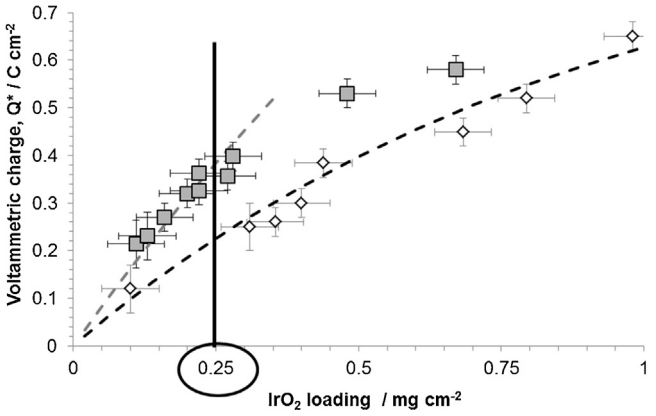

Fig. 6. Evolution of the total voltammetric charge of IrO_2 and 50 wt.% IrO_2/Ti anodes with IrO_2 loading. Doted lines are the result of the model presented in the first part of this paper [38].

the method proposed by Lodi et al. [39]. The evolution of the total voltammetric charge Q* of unsupported IrO_2 and of 50 wt.% IrO_2/Ti anodes *vs.* IrO_2 loading are plotted on Fig. 6. For both anodes, Q* logically increases with the IrO_2 loading. However, for the same IrO_2 loading, Q* is larger for IrO_2/Ti than for unsupported IrO_2. This difference is attributed to the presence of conductive titanium particles that improve electronic conduction between IrO_2 particles among the catalyst layer. More IrO_2 catalytic sites are probed when Ti is added.

In the first part of this research paper, a simple model was used to fit experimental data [38]. In this model, the anodic layer was considered as a stacking of catalyst particles of similar shape and size. The electrochemical sites of the first layer of IrO_2 nanoparticles (in direct contact with the membrane) were assumed to be 100% active. The fraction of active sites of the second layer depends on the covering by the first layer and so on for the successive layers. The activity of any layer within this stacking of catalyst particles depends on its covering by other layers. The total voltammetric charge of electrodes (noted Q*), was expressed as:

$$Q^* = B \times \exp\left(-\frac{1}{A}\right)\left(\frac{1-\exp\left(-C\frac{m_{iro_2}}{RA}\right)}{1-\exp\left(-\frac{1}{A}\right)}\right) \quad (1)$$

where A is a factor which expresses the efficiency of one layer in the stacking, B corresponds to the voltammetric charge of one unique layer of catalyst nanoparticles, m_{IrO_2} is the IrO_2 loading in g m^{-2},

Table 1
Best fit values of parameters A and B.

Electrodes	A (a.u.)	B (C)
Pure IrO_2	86	125
50 wt.% IrO_2/Ti	120	180

and R the radius of IrO_2 nanoparticles. C is a constant used to model other sphere packing (cubic, hexagonal, tetrahedral etc. . .).

$$C = \frac{3\sqrt{3}}{2\pi\rho} \quad (2)$$

ρ is the volumetric weight of iridium oxide ($\rho = 11.66\ g\ cm^{-3}$ [40]).

Experimental plots of Q* *vs.* IrO_2 loading (Fig. 6) have been fitted with Eq. (1). Parameters A and B have been determined by iteration. Best fits are compiled in Table1.

This model, based on several simplifying geometrical assumptions listed in the first part of this research paper was found sufficiently elaborated to account for the experimental relationship between Q* and IrO_2 loading for unsupported IrO_2 electrodes. For the 50 wt.% IrO_2/Ti electrodes, two different domains have been identified. First, at low IrO_2 loadings (<0.25 mg cm^{-2}), when titanium particles protrude from the active layer and when Q* is significantly enhanced compared to what is obtained with unsupported IrO_2 catalyst layers. Second, for IrO_2 loading higher than 0.25 mg cm^{-2}, the evolution of Q* *vs.* IrO_2 loading becomes quite similar to what is obtained with unsupported IrO_2 catalyst. This is an indication that the benefit of adding titanium particles declines when the IrO_2 loading is increased.

We can see from Table 1 that factors A and B are both much higher for 50 wt.% IrO_2/Ti electrodes than for unsupported IrO_2 electrodes. These differences can be attributed to a better dispersion of IrO_2 nanoparticles in the IrO_2/Ti mixture and an improvement of the catalyst efficiency in the entire thickness of the electrode. In addition, titanium micro-sized particles can act as an extension on the current collector and thus improve electrical conduction in both surface and volume regions of the electrode.

3.3. PEM water electrolysis performance

The electrochemical performances of the different MEAs containing different IrO_2 loadings were measured during PEM water electrolysis experiments conducted at current densities up to 2 A cm^{-2}. Some typical polarization curves are plotted on Fig. 7a. By increasing the IrO_2 loading (unsupported IrO_2) from 0.10 to 0.40 mg cm^{-2} the level of performance is significantly increased. For higher loadings, performances tend to reach a limit. When IrO_2/Ti mixtures are used, the situation is different. Results obtained with 0.12 mg cm^{-2} IrO_2/Ti (the lowest IrO_2 loading tested in this study) are also plotted for comparison. The benefit of adding titanium particle to the catalyst layer is clearly demonstrated. A cell voltage of only 1.73 V was measured at 1 A cm^{-2} and 80 °C (η = 72% LHV), roughly similar to the voltage reached by using 0.4–0.7 mg cm^{-2} of unsupported IrO_2. In comparison, when a loading of 0.10 mg cm^{-2} of unsupported IrO_2 is used, the cell voltage is 1.89 V (η = 66% LHV) at 1 A cm^{-2} and 80 °C.

Addition of titanium particles has therefore a direct and positive effect on the electroactive surface area of the catalyst layer (at least for low IrO_2 loadings <0.25 mg cm^{-2}). It also has a significant impact on the ohmic resistance of the MEA (which is given by the slope of the polarization curves). Since the same membrane was used for all experiment, the benefit was attributed to more conducting catalytic layers. However, the measurement of electronic conductivity of powders or mixture of powders embedded in a polymer matrix (using for example a probe technique) is not a trivial task. Significantly scattered data sets have been obtained on our samples.

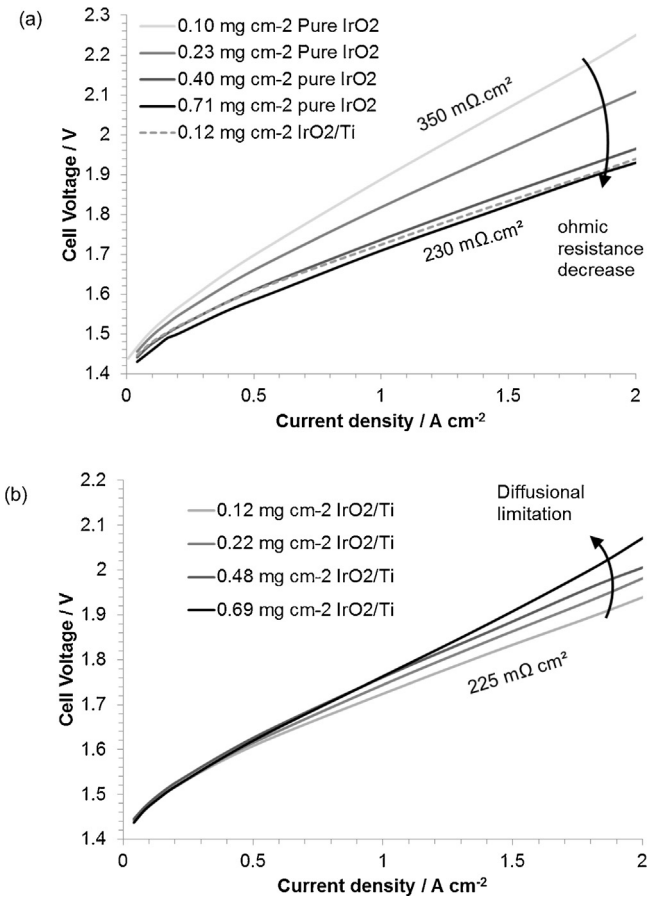

Fig. 7. Effect of the IrO_2 loading on the PEMWE cell performance at 80 °C. (a) Comparison of polarization curves obtained with different loadings of pure IrO_2 and a curve obtained with IrO_2/Ti 50 wt.% (0.12 mg cm^{-2} IrO_2). (b) Polarization curves obtained with different loadings of IrO_2 using IrO_2/Ti 50 wt.% in the active layer.

Hence, it was not possible to measure accurately enough the electronic conductivity of IrO_2 and IrO_2/Ti catalytic layers to quantify the gain provided by the addition of Ti.

Fig. 7b shows that an increase of the IrO_2 loading when the IrO_2/Ti 50 wt.% mixture is used as anodic material does not always improve the electrochemical performances. On the contrary, the cell voltage tends to increase, particularly at high current density. This is a possible indication that diffusional limitations are appearing. We believe that this phenomenon is directly related to the thicker catalyst layers that tend to introduce mass transport limitations of evolving oxygen.

In order to gain a better understanding on the influence of the IrO_2 loading (with and without titanium nanoparticles) on (i) charge transfer kinetics and (ii) ohmic resistance of the catalytic layer, the cell voltages measured at two different current densities have been compared:

- The cell voltage at 0.12 A cm^{-2} (Fig. 8a): at low current density, the voltage drop due to the ohmic resistance of the cell is negligible; mainly charge transfer effects contribute to the polarization curve.
- The cell voltage at 1 A cm^{-2} (Fig. 8b): at high current density, charge transfer resistance are small and the voltage drop due to the internal cell resistance is predominant; this is a domain that provides information on electronic conduction of the catalytic layer and contact resistance between catalyst and porous current collector.

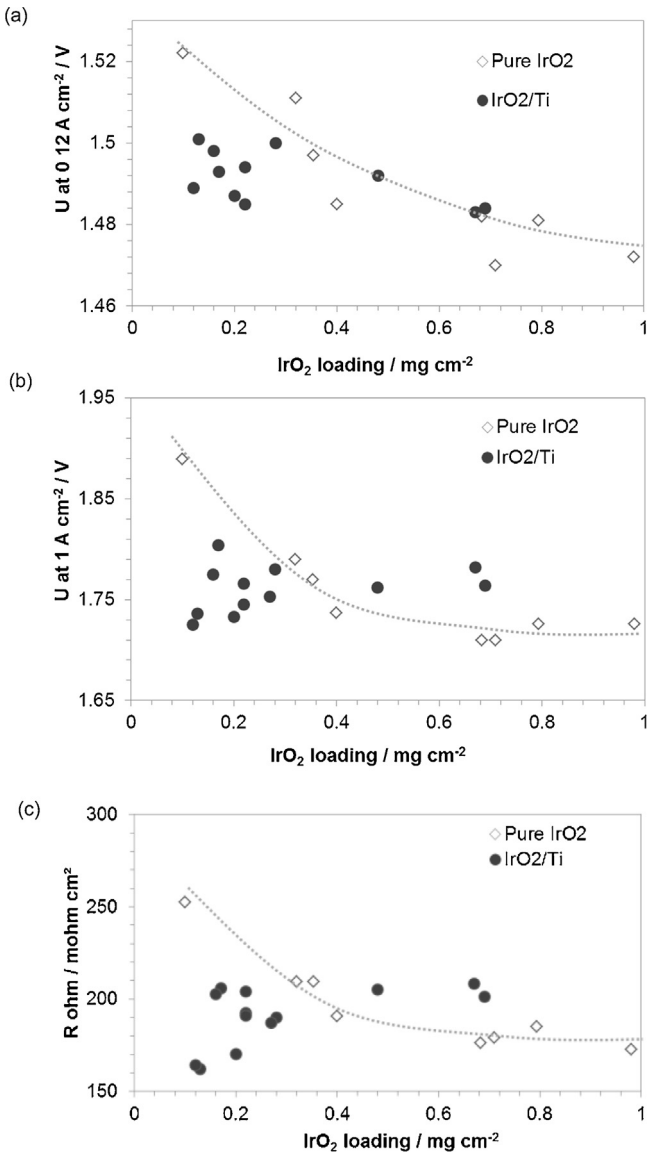

Fig. 8. Evolution of the cell voltage at (a) 0.12 A cm^{-2} and (b) 1 A cm^{-2} and the ohmic resistance as a function of the IrO_2 loading at 80 °C.

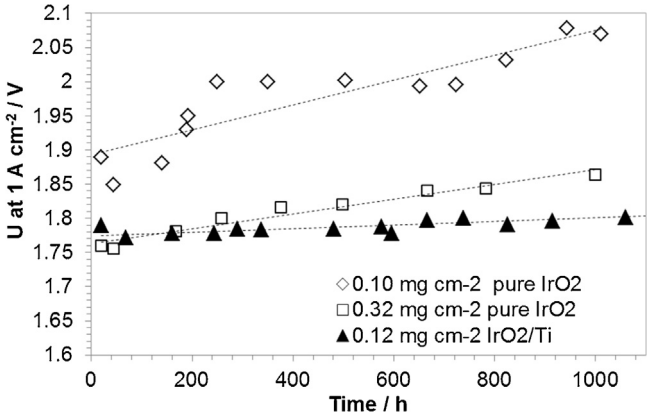

Fig. 9. Measured cell voltage evolution during "accelerated" ageing test at 1 A cm^{-2} on very low IrO_2 loading MEAs (pure IrO_2 and 50 wt. % IrO_2/Tianode) as a function of time at 80 °C.

At low current density (see Fig. 8a), the positive effect resulting from the addition of titanium micro-particles is observed mainly at low IrO_2 loadings (<0.25 mg cm^{-2}). This is a confirmation of the results obtained by cyclic voltammetry. For higher loadings, no additional positive effect is gained. In such cases, titanium particles are partly or fully embedded within the catalyst layers, with no significant advantage.

At high current density (Fig. 8b), the addition of titanium microparticles has a positive effect up to 0.5 mg cm^{-2}. As discussed in the first part of this research paper [38], when the catalyst loading is less than 0.5 mg_{IrO_2} cm^{-2}, a lack of electrical percolation is observed at the surface of the membrane. The addition of titanium particles as conductive support favors the electronic conduction within the catalyst layer and reduces the cell voltage at high current density. For loadings above 0.5 mg_{IrO_2} cm^{-2}, the ohmic resistance of catalyst layers containing titanium microparticles tend to exceed that of unsupported IrO_2 (Fig. 8c). Above the percolation threshold of IrO_2 nanoparticles, the addition of titanium particles does not bring any advantage; it only increases the thickness of the anodic layer and thus increases its ionic and electronic resistance, a situation which in turn has a negative impact on mass transport phenomena.

Effect of the titanium particles on the performance is probably highly dependent on several parameters such as the Ti particle average size, the size distribution and the IrO_2/Ti ratio. Further work is required to identify the most appropriate titanium particle size that should reduce the scattering of data observed at high current density and facilitate operation with low IrO_2 loading (Fig. 8b and c).

3.4. Durability of MEAs with low IrO_2 loading

Addition of titanium microparticles to the catalyst layer of a PEMWE anode looks to be a very simple and cost effective solution to significantly reduce the IrO_2 loading whilst maintaining a high level of performance. However, to confirm the interest of adding titanium, it is necessary to determine whether these microparticles are stable enough in the highly aggressive environment of a PEMWE anode or not. The risk is that the long-term oxidation of the titanium microparticles canincrease the electrical resistance of the electrode and reduce the performance of the cell.

Three different water electrolysis ageing tests (1000 h each) were conducted in order to assess the stability of the very low catalyst loading MEAs (0.1 mg cm^{-2} IrO_2) using the "accelerated" ageing test described in the experimental section. The time evolution of the cell voltages of two MEAs prepared with pure IrO_2 particles (loadings of 0.10, 0.32 mg cm^{-2} IrO_2 respectively) and a MEA prepared with 50 wt.% IrO_2/Ti (0.12 mg cm^{-2} IrO_2) measured at 1 A cm^{-2} are plotted on Fig. 9.

Results show that the cell voltage of the 50 wt.% IrO_2/Ti MEA remains close to the initial value of 1.78 V, without any significant cell voltage degradation over the 1000 h of operation at 80 °C (a degradation rate of approximately 27 μV h^{-1} is measured). By comparison, results obtained with the pure IrO_2 particles catalyst layer (same catalyst loading) show lower performance: the cell voltage is 1.9 V at 1 A cm^{-2} and 80 °C. Moreover, this catalyst layer (with a very low loading of unsupported IrO_2) is not very stable: the cell voltage fluctuates during the test and increases at an average rate close to 180 μV h^{-1}. To reach the same voltage as the IrO_2/Ti MEA, it is necessary to increase the catalyst loading of the pure IrO_2 electrode up to 0.3 mg cm^{-2}. However, even with such loading, the catalyst layer is still not sufficiently stable (the cell voltage was found to increase at a rate of 110 μV h^{-1}).

A deeper investigation of degradation processes reveals that the increase of the cell voltage was due to both an increase of the purely ohmic resistance of the cell (current collectors, membrane,

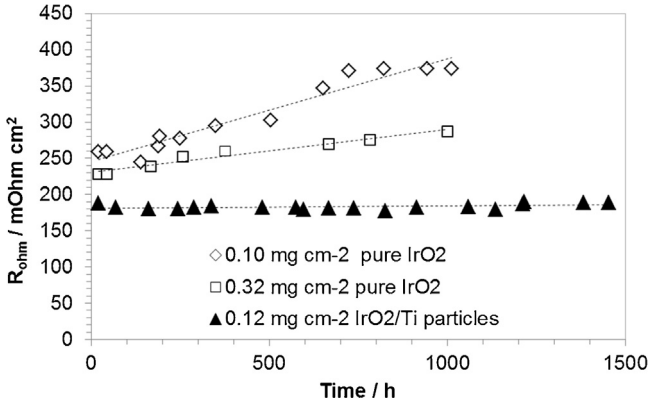

Fig. 10. Measured cell voltage evolution during "accelerated" ageing test at 1 A cm^{-2} and 80 °C on very low IrO_2 loading MEAs (pure IrO_2 and 50 wt. % IrO_2/Ti anode).

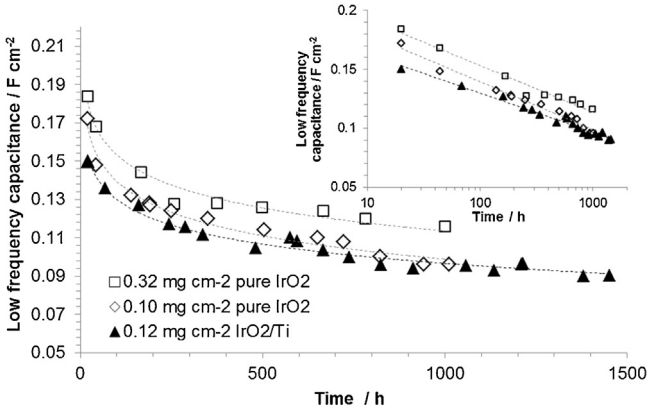

Fig. 11. Evolution of the capacitance value of the low frequency electrical contribution with ageing time ("accelerated" ageing test, 80 °C). Inset: same values drawn *vs.* time in log scale.

electrodes) and an increase of the charge transfer resistance. As shown on Fig. 10, the purely ohmic resistance of the cell increases rapidly for the 0.10 mg cm^{-2} pure IrO_2 MEA (141 μΩ cm^2 h^{-1}). This increase is significantly reduced for the 0.32 mg cm^{-2} pure IrO_2 MEA (59 μΩ cm^2 h^{-1}), whereas on the 0.12 mg cm^{-2} IrO_2/Ti MEA, the cell resistance remains quite constant (3 μΩ cm^2 h^{-1}) over more than 1'500 h of operation.

The rate at which the purely ohmic resistance of the cell and the charge transfer resistance (determined from EIS measurements) increase along the ageing tests are reported in Table 2. Results clearly show that the degradation of pure IrO_2 MEAs is mainly due to an increase of the ohmic resistance of the catalyst layer. During the test, the surface of the porous current collectors is oxidized and the contact resistance with the catalyst layer increases even more when the cell voltage increases. Addition of titanium microparticles tend to improve the electronic conductivity of the electrode and to prevent the oxidation of the titanium current collector by maintaining a low cell voltage (less than 2 V at 2 A cm^{-2}) and reducing the amount of heat dissipated by Joule effect.

It was also observed during the tests that the capacitance values measured by EIS at low frequency decreases significantly. Results obtained with three different IrO_2 loadings are plotted in Fig. 11. The same trend was observed for every sample whether containing pure IrO_2 or supported IrO_2/Ti catalyst. The capacitance was found to decrease linearly with the logarithm of time.

A good correlation is found between this low frequency capacitance and the total voltammetric charge (Q*) of the electrodes determined by cyclic voltammetry (see Fig. 12). Therefore, the low frequency capacitance can be considered as representative of the electrochemical surface area of the anode. When the low frequency capacitance decreases along the ageing test, this is an indication that the number of active sites at the anode is also decreasing.

The "solar-type" ageing test is significantly less aggressive than the "accelerated" ageing test (temperature of 60 °C and current density limited to 1.7 A cm^{-2}) but closer to practical applications. This second ageing test was conducted for 1'500 h using a MEA that contained 0.16 mg_{IrO_2} cm^{-2} of Ti supported IrO_2 (50 wt.% IrO_2/Ti). The degradation rate of 2 μV h^{-1} at 1 A cm^{-2} was found very low com-

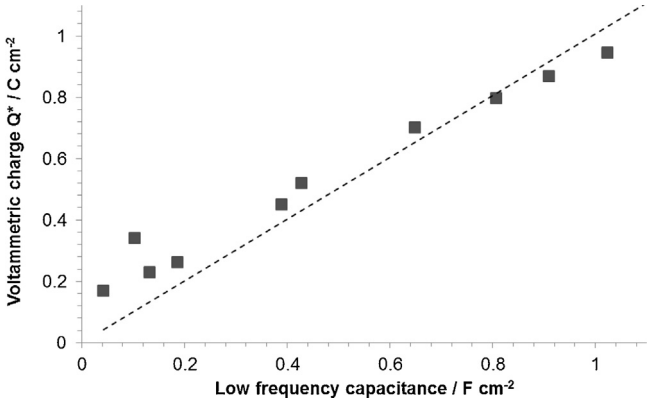

Fig. 12. Relationship between the total charge (Q*) measured on the electrodes by cyclic voltammetry and the low frequency capacitance calculated by fitting of EIS measurements.

pared to the "accelerated" ageing test. However, it can be observed on Fig. 13 that the decrease of the low frequency capacitance during the "solar-type" ageing test is similar to what is observed during the "accelerated" ageing test. Then, this apparent loss in the electrochemical surface area cannot be directly correlated with the degradation of performance and is not depending on the operating conditions (temperature, maximum cell voltage).

The performance level of this MEA made with IrO_2/Ti and low IrO_2 loading (0.16 mg_{IrO_2} cm^{-2}) was compared to a conventional MEA containing 1.6 mg cm^{-2} of unsupported IrO_2. This ageing test was continued up to 6500 h (Fig. 14). It appears that this conventional MEA presents the same degradation rate as the previous one (3 μV h^{-1}) and an equivalent loss in the capacitance value (1/3 of the initial value is lost during the first 1000 h of the test). This is a confirmation of the positive effect of the addition of titanium particles, even during long-term operation.

Finally, it is interesting to note that during this long ageing test, the value of R_{ohm} tends to decrease at a rate of approximately 2 μΩ cm^2 h^{-1}. This is possibly due to the thinning of the Nafion

Table 2
Values of resistance variation during "accelerated" ageing test at 80 °C calculated from EIS measurements. Purely ohmic resistance of the cell Rohm and charge transfer resistance R_{CT}.

Electrodes	R_{ohm} (μΩ cm^2 h^{-1})	R_{CT} (μΩ cm^2 h^{-1})	Degradation rate at 1 A cm^{-2} (μV h^{-1})
0.10 mg cm^{-2} pure IrO_2	141	43	180
0.32 mg cm^{-2} pure IrO_2	59	45	110
0.12 mg cm^{-2}, 50 wt.% IrO_2/Ti	3	25	27

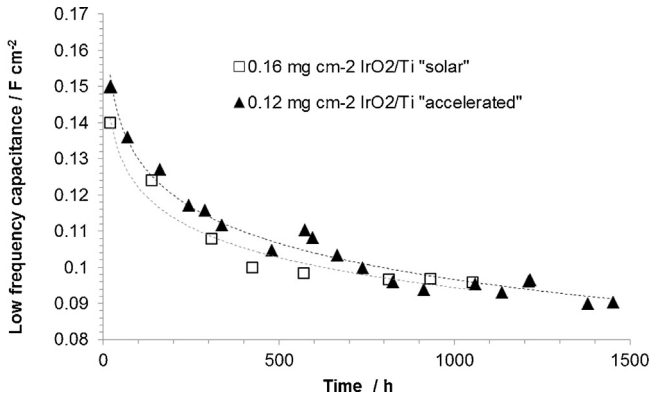

Fig. 13. Evolution of the capacitance value of the low frequency electrical contribution with ageing time for two MEAs tested using the "accelerated" ageing test at 80 °C and the "solar-type" ageing test at 60 °C.

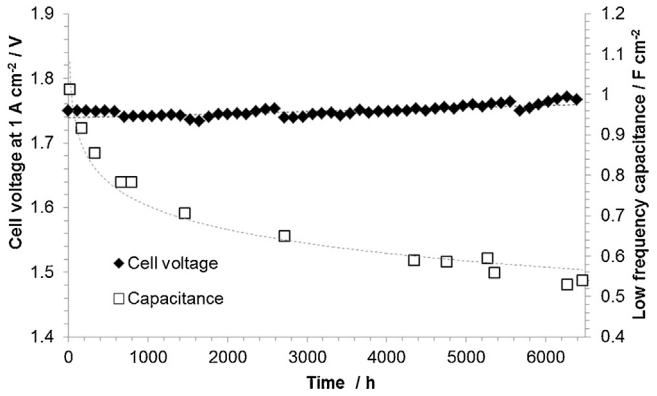

Fig. 14. Measured cell voltage evolution during "solar-type ageing test at 1 A cm^{-2} and 60 °C on a 1.6 mg cm^{-2} pure IrO_2 MEA. Secondary axis: evolution of the low frequency capacitance with ageing time.

membrane during cycling, as already reported elsewhere [41,42], and as observed by post-mortem SEM observations. This gradual reduction of the ionic resistance of the membrane tends to partly compensate the increase of the electronic cell resistance due to titanium oxidation.

4. Conclusions

The work reported in this research work demonstrates that micro-sized titanium particles are promising support materials for IrO_2 in PEM water electrolysis cells. When the IrO_2 loading of the anode is less than 0.5 mg_{IrO_2} cm^{-2}, performances of the cell using a supported IrO_2/Ti catalyst (50 wt.% IrO_2) are higher compared to those obtained with unsupported IrO_2. This result is explained by the fact that titanium particles protruding from the electrode surface can fit inside the surface pores of the current collector and contribute to facilitate electron transfer to and within the catalyst layer, hence optimized the amount of electrochemically active IrO_2 sites.

Two different long-term ageing tests have been used to evaluate the stability of the IrO_2/Ti catalyst layers and to compare their level of performance with MEAs that contain only pure IrO_2. These tests confirmed the benefit of adding these micro-sized titanium particles, especially to stabilize the level of performance of (very) low catalyst loadings (at least for the 1'500 h of the tests).

A detailed analysis of the electrical properties of the PEM cells during these ageing tests revealed that three main different electrical factors contribute to the degradation of MEA performances: the purely ohmic resistance (R_{ohm}) of the cell, the charge transfer resistance (R_{CT}) of the anode and the capacity measured at low frequency (this capacity is related to the electrochemically active surface area of the electrodes). This study based on a simple phenomenological approach allows us to identify the main degradation processes taking place in the PEM cell:

- When the cell is operated at low temperature (60 °C), the purely ohmic part of the impedance (R_{ohm}) remains quite stable or even tend to slightly decrease during the ageing tests (this is possibly due to the membrane thinning).
- When the cell is operated at higher temperature (80 °C) both the ohmic resistance (R_{ohm}) and the charge transfer resistance (R_{CT}) increase linearly with time. These rates are even greater when the cell voltage exceeds the value of 2 V during operation (this was observed on low performance MEAs prepared with low catalyst loading and pure IrO_2 powder). The degradation of the polarization resistance is attributed to the oxidation of the titanium current collectors and the resulting increase of the contact resistance between this material and the catalyst layer.
- A general trend is that the capacity measured at low frequency (which is related to the electrochemically active surface area of the catalytic layer) was found to decrease quickly during the first hours of operation and then tend to reach a constant value. This trend seems independent of any operating parameter (temperature, cycle profile, catalyst loading,. . .). Such a decrease of the electrochemically active surface area is attributed to the stress produced by oxygen nucleation within the porous catalyst layer, by bubbling and by erosion of the catalyst particles by water flowing.

The addition of micro-sized titanium particles to the anodic catalyst layer appears to be a very simple and efficient way to significantly reduce noble metals loadings in PEMWE cells while maintaining at the same time a high level of performance (both low cell voltage and extended durability). However, further work is still required to optimize titanium particles size and to maximize the electrochemical benefit that can be gained from this additive.

Acknowledgements

The authors want to acknowledge the financial support from the ANR (French National Research Agency) in the framework of the AITOILES project (ANR-11-PRGE-0001).

References

[1] F. Barbir, PEM electrolysis for production of hydrogen from renewables sources energies, Sol. Energy 78 (2005) 661–669.
[2] R.S. Liu, L. Zhang, X. Sun, H. Liu, J. Zhang, Electrochemical Technologies for Energy Storage and Conversion, John Wiley, 2012, http://dx.doi.org/10.1002/9783527639496.
[3] E. Rasten, Electrocatalysis in water electrolysis with solid polymer electrolyte, PhD Thesis, Norwegian University of Science and Technology, 2001. <http://www.diva-portal.org/smash/get/diva2:121826/FULLTEXT01pdf> (accessed 01.02.13).
[4] E. Rasten, G. Hagen, R. Tunold, Electrocatalysis in water electrolysis with solid polymer electrolyte, Electrochim. Acta 48 (2003) 3945–3952, http://dx.doi.org/10.1016/j.electacta.2003.04.001.
[5] S.-Y. Huang, P. Ganesan, H.-Y. Jung, B.N. Popov, Development of supported bifunctional oxgen electrocatalysts and corrosion-resistant gas diffusion layer for unitized regenerative fuel cell applications, J. Power Sources 198 (2012) 23–29.
[6] J. Xu, G. Liu, J. Li, X. Wang, The electrocatalytic properties of an IrO_2/SnO_2 catalyst using SnO_2 as a support and an assisting reagent for the oxygen evolution reaction, Electrochim. Acta 59 (2012) 105–112, http://dx.doi.org/10.1016/j.electacta.2011.10.044.
[7] S. Siracusano, N. Van Dijk, E. Payne-Johnson, V. Baglio, S. Aricò, Nanosized IrOx and IrRuOx electrocatalysts for the O_2 evolution reaction in PEM water electrolysers, Appl. Catal. B Environ. 164 (2015) 488–495, http://dx.doi.org/10.1016/j.apcatb.2014.09.005.
[8] N. Mamaca, E. Mayousse, S. Arrii-Clacens, T.W. Napporn, K. Servat, N. Guillet, et al., Electrochemical activity of ruthenium and iridium based catalysts for

oxygen evolution reaction, Appl. Catal. B Environ. 111–112 (2012) 376–380, http://dx.doi.org/10.1016/j.apcatb.2011.10.020.
[9] E. Antolini, Carbon supports for low-temperature fuel cell catalysts, Appl. Catal. B Environ. 88 (2009) 1–24, http://dx.doi.org/10.1016/j.apcatb.2008.09.030.
[10] S.A. Grigoriev, V.N. Fateev, H. Middleton, T.O. Saetre, P. Millet, A comparative evaluation of palladium and platinum nanoparticles as catalysts in proton exchange membrane electrochemical cells, Int. J. Nucl. Hydrog. Product. Appl. 1 (2008) 343–354.
[11] S.A. Grigoriev, P. Millet, V.N. Fateev, Evaluation of carbon-supported Pt and Pd nanoparticles for the hydrogen evolution reaction in PEM water electrolysers, J. Power Sources 177 (2008) 281–285, http://dx.doi.org/10.1016/j.jpowsour.2007.11.072.
[12] S.A. Grigoriev, V.I. Porembskiy, S.V. Korobtsev, V.N. Fateev, F. Auprêtre, P. Millet, High-pressure PEM water electrolysis and corresponding safety issues, Int. J. Hydrogen Energy 36 (2011) 2721–2728, http://dx.doi.org/10.1016/j.ijhydene.2010.03.058.
[13] A.J. Bard, R. Parson, J. Jordan, Standard Potentials in Aqueous Solution, Monographs in Electroanalytical Chemistry and Electrochemistry, CRC Press, New York United States, 1985.
[14] P.N. Ross, The corrosion of carbon black anodes in alkaline electrolyte, J. Electrochem. Soc. 131 (1984) 1742, http://dx.doi.org/10.1149/1.2115953.
[15] L.R. Ma, S. Sui, Y.C. Zhai, Investigations on high performance proton exchange membrane water electrolyzer, Int. J. Hydrogen Energy 34 (2009) 678–684, http://dx.doi.org/10.1016/j.ijhydene.2008.11.022.
[16] J. Polonský, I.M.M. Petrushina, E. Christensen, K. Bouzek, C.B.B. Prag, J.E.T.E.T. Andersen, et al., Tantalum carbide as a novel support material for anode electrocatalysts in polymer electrolyte membrane water electrolysers, Int. J. Hydrogen Energy 37 (2012) 2173–2181, http://dx.doi.org/10.1016/j.ijhydene.2011.11.035.
[17] A.V. Nikiforov, A.L. Tomas Garcia, I.M. Petrushina, E. Christensen, N.J. Bjerrum, Preparation and study of IrO_2/SiC–Su supported anode catalyst for high temperature PEM steam electrolysers, Int. J. Hydrogen Energy 36 (2011) 5797–5805.
[18] C. Chen, H. Waraksa, D. Cho, EIS studies of porous oxygen electrodes with discrete particles-I. Impedance of oxide catalyst supports, J. Electrochem. Soc. 150 (2003) E423–E428, http://dx.doi.org/10.1149/1.1594729.
[19] S. Siracusano, V. Baglio, C. D'Urso, A.S. Aricò, Preparation and characterization of titanium suboxides as conductive support of IrO_2 electrocatalysts for application in SPE electrolysers, Electrochim. Acta 54 (2009) 6292–6299.
[20] G. Chen, S.R. Bare, T.E. Mallouk, Development of supported bifunctional electrocatalysts for unitized regenerative fuel cells, J. Electrochem. Soc. 149 (2002) A1092, http://dx.doi.org/10.1149/1.1491237.
[21] L. Vazquez-Gomez, S. Ferro, A. De Battisti, Preparation and characterization of RuO_2–IrO_2–SnO_2 ternary mixtures for advanced electrochemical technology, Appl. Catal. B Environ. 67 (2006) 34–40, http://dx.doi.org/10.1016/j.apcatb.2006.03.023.
[22] M. Miu, I. Kleps, M. Danila, T. Ignat, M. Simion, A. Bragaru, et al., Electrocatalytic activity of platinum nanoparticles supported on nanosilicon, Fuel Cells (2010) 259–269, http://dx.doi.org/10.1002/fuce.200900202.
[23] M. Yagi, E. Tomita, S. Sakita, T. Kuwabara, K. Nagai, Self-assembly of active IrO_2 colloid catalyst on an ITO electrode for efficient electrochemical water oxidation, J. Phys. Chem. B 109 (2005) 21489–21491, http://dx.doi.org/10.1021/jp0550208.
[24] A.A. Gusev, E.G. Avvakumov, A.Z. Medvedev, A.I. Masliy, Ceramic electrodes based on magneli phases of titanium oxides, Sci. Sinter 39 (2007) 51–57.
[25] H.B. Beer, Electrode and coating therefor, US 3,632,498, 1972.
[26] C. Comninellis, G. Vercesi, Characterization of DSA®-type oxygen evolving electrodes: choice of a coating, J. Appl, Electrochem. 21 (1991) 335–345, <http://www.springerlink.com/index/P70U654625160071pdf> (accessed 04.03.13).
[27] R.S. Liu, L. Zhang, X. Sun, H. Liu, J. Zhang, Electrochemical Technologies for Energy Storage and Conversion, WILEY-VCH Verlag, 2012, http://dx.doi.org/10.1002/9783527639496.
[28] S. Trasatti, Electrocatalysis in the anodic evolution of oxygen and chlorine, Electrochim. Acta 29 (1984) 1503–1512, http://dx.doi.org/10.1016/0013-4686(84)85004-5.
[29] S. Trasatti, Electrocatalysis: understanding the success of DSA®, Electrochim. Acta. 45 (2000) 2377–2385, http://dx.doi.org/10.1016/S0013-4686(00)338-8.
[30] D.M. Brunette, P. Tengvall, M. Textor, P. Thomsen, Titanium in Medicine, Springers, 2001.
[31] J. Krýsa, R. Mráz, I. Roušar, Corrosion rate of titanium in H2SO4, Mater. Chem. Phys. 48 (1997) 64–67, http://dx.doi.org/10.1016/s0254-0584(97)80079-x.
[32] S.A. Fadl-allah, Q. Mohsen, Characterization of native and anodic oxide films formed on commercial pure titanium using electrochemical properties and morphology techniques, Appl. Surf. Sci. 256 (2010) 5849–5855, http://dx.doi.org/10.1016/j.apsusc.2010.03.058.
[33] P. Mazúr, J. Polonský, M. Paidar, K. Bouzek, Non-conductive TiO_2 as the anode catalyst support for PEM water electrolysis, Int. J. Hydrogen Energy 37 (2012) 12081–12088, http://dx.doi.org/10.1016/j.ijhydene.2012.05.129.
[34] S. Siracusano, V. Baglio, R.O. Stassi, V.A. rnelas, S. Aricò, Investigation of IrO_2 electrocatalysts prepared by a sulfite-couplex route for the O_2 evolution reaction in solid polymer electrolyte water electrolyzers, Int. J. Hydrogen Energy 36 (2011) 7822–7831, http://dx.doi.org/10.1016/j.ijhydene.2010.12.080.
[35] G. Li, H. Yu, W. Song, X. Wang, Y. Li, Z. Shao, et al., Zeolite-templated IrxRu1–xO2 electrocatalysts for oxygen evolution reaction in solid polymer electrolyte water electrolyzers, Int. J. Hydrogen Energy 37 (2012) 16786–16794, http://dx.doi.org/10.1016/j.ijhydene.2012.08.087.
[36] M. Yamaguchi, K. Okisawa, T. Nakanori, Development of high performance solid polymer electrolyte water electrolyzer in WE-NET, in: Energy Convers. Eng. Conf. 1997. IECEC-97, Proc. 32nd Intersoc., 1965, pp. 1958–1965, <http://ieeexplore.ieee.org/xpls/abs_all.jsp?arnumber=656726> (accessed February 1, 2013).
[37] S. Trasatti, G. Buzzanca, Ruthenium dioxide: a new interesting electrode material. Solid structure and electrochemical behaviour, J. Electroanal. Chem. Interfacial Electrochem. 29 (1971) A1–A5, http://dx.doi.org/10.1016/S0022-0728(71)80111-0.
[38] C. Rozain, E., Mayousse, N., Guillet, P. Millet, Influence of iridium oxide loadings on the performance of PEM water electrolysis cells: Part I - Pure IrO_2-based anodes, Appl. Catal. B: Environ., submitted.
[39] G. Lodi, E. Sivieri, A. Debattisti, S. Trasatti, Ruthenium dioxide-based film electrodes. 3. Effect of chemical composition and surface morphology on oxygen evolution in acid-solutions, J. Appl. Electrochem. 8 (1978) 135–143, http://dx.doi.org/10.1007/bf00617671.
[40] Handbook of Chemistry and Physics, in: R.C. West (Ed.), 56th ed., CRC Press, Cleveland, Ohio, 1975.
[41] S. Stucki, G.G. Scherer, PEM water electrolysers: evidence for membrane failure in 100 kW demonstration plants, J. Appl. Electrochem. 28 (1998) 1041–1049, <http://www.springerlink.com/index/u126m62g76768751pdf> (accessed 01.02.13).
[42] M. Chandesris, V. Médeau, N. Guillet, S. Chelghoum, D. Thoby, F. Fouda-Onana, Membrane degradation in PEM water electrolyzer: numerical modeling and experimental evidence of the influence of temperature and current density, Int. J. Hydrogen Energy 40 (2014) 1353–1366, http://dx.doi.org/10.1016/j.ijhydene.2014.11.111.